# Estimation of Hankinson's formula coefficient for elastic wave transmission velocity of red pine by the indirect method

*HyeongJun Han*†
Timber Engineering Laboratory
Department of Forest Products Engineering
Chungbuk National University
Cheongju, Republic of Korea
E-mail: 2024247003@chungbuk.ac.kr

*KyoungHyun Ryu*†
Timber Engineering Laboratory
Department of Forest Products Engineering
Chungbuk National University
Cheongju, Republic of Korea
E-mail: wokohyun@chungbuk.ac.kr

*KugBo Shim*†*
Professor of Forest Products Engineering
Timber Engineering Laboratory
Department of Forest Products Engineering
Chungbuk National University
Cheongju, Republic of Korea
E-mail: kbshim@chungbuk.ac.kr

(Received 10 August 2025)

**Abstract:** This study determined the Hankinson's formula coefficient *n* for red pine (*Pinus densiflora*) using the indirect elastic wave transmission test under varying moisture contents (12%, 15%, and 18%). Hankinson's formula is a mathematical relationship used to predict the mechanical properties of wood at any angle relative to the grain. With information on the elastic wave transmission speed parallel (P, 0°) and perpendicular (Q, 90°) to the fiber direction, the wave transmission speed at intermediate angles can be predicted using Hankinson's formula. A visually defect-free 81- to 90-year red pine board (400 × 400 × 50 mm) was selected as the test specimen. The moisture content of specimens was adjusted to 12%, 15%, and 18%. Coefficient *n* of Hankinson's formula, was calculated by taking measurements were taken at grain angles of 0°, 15°, 30°, 45°, 60°, 75°, and 90° using both ultrasonic and stress waves by the indirect transmission method.
The coefficients (*n*) obtained from ultrasonic wave measurements were 2.0, 1.9, and 1.9 at 12%, 15%, and 18% moisture contents, respectively. The values determined from stress wave measurements were 1.7, 1.7, and 1.6 at the same moisture contents, respectively. These results indicate that the transmission path of elastic waves in red pine can be effectively modeled using the coefficient *n* from Hankinson's formula, which varies with moisture content. This suggests the potential applicability of the formula in evaluating internal defects or decay in wood through quantitative wave-based analysis.

**Keywords:** Nondestructive test; Ultrasonic wave; Stress wave; Indirect method; Hankinson's formula; *Pinus densiflora*

## Introduction

Wood is an organic material that varies in moisture content based on the surrounding environment. High moisture wood contents favor insect and fungal attack. Insect activity within the wood causes structural damage that is often hidden from view and may not be detected until significant destruction has occurred (Verbist et al. 2019). This reduces the strength of wooden structural members, leading to overall damage in wooden buildings (Ghaly and Edwards 2011; Wang et al. 2018). Damage caused by termites is increasing due to climate change (Buczkowski and Bertelsmeier 2017; Lee et al. 2021).

The carbon emission reduction benefits of wooden structures for carbon neutrality increase with long-term use of wood (Churkina et al. 2020; Starzyk et al. 2024). To ensure the long-term use of wooden structures, it is essential to evaluate the

* Corresponding author
† Society of Wood Science & Technology member

strength of structural members. Strength evaluation methods are divided into destructive and nondestructive techniques. Destructive testing damages the material and can render it unsuitable for prolonging building life (Shabani et al. 2020). In contrast, nondestructive methods can predict strength without damaging the material, making them ideal for preserving wooden structures, cultural heritage sites, or for safety evaluations of existing buildings (Riggio et al. 2014).

Therefore, to extend the lifespan of wooden structures, nondestructive evaluation methods should be applied. Additionally, safety assessment protocols based on the degree of deterioration need to be established.

Various nondestructive testing methods for wooden structures have relied on experience, such as craftsmen's intuitive judgment, visual inspection, and tapping tests that diagnose through the sound produced by tapping wood (Azzi et al. 2025). Such empirical diagnoses lack accuracy and consistency, and thus lack a scientific basis for safety assessment of wooden structures (Kim et al. 2003). Therefore, a quantitative evaluation method using nondestructive testing is needed.

Currently, the most commonly used nondestructive testing methods include drilling resistance tests, X-rays, and elastic wave nondestructive tests (Ondrejka et al. 2020). Among these, nondestructive tests using elastic waves are advantageous for field application because the test process is fast and simple (Zielińska and Rucka 2021). This method measures the time of flight (ToF) for elastic waves to penetrate the interior of a member and calculates the transmission speed to detect decay and defects. The transmission speed of elastic waves is affected by the moisture content in the wood. As wood moisture content increases, the stiffness decreases (Kretschmann 2010), and the transmission speed of elastic waves slows (Montero et al. 2015; Yang et al. 2015).

Many studies have been conducted to detect internal decay using elastic nondestructive testing (Niederleithinger and Vössing 2018). However, most studies have been conducted using the direct measurement method, where transducers are placed face to face and measured. Since this direct measurement method is difficult to apply when the opposite side of the wood used in a wooden structure is not exposed, research on the indirect method, where the transducers are placed side by side and measured, is necessary.

The propagation of elastic waves through wood follows the fastest path between the transmitter and receiver (Figure 1, Path A). When decay or defects are present, the elastic waves detour around the cavity and travel along the fastest available path (Figure 1, Path B). As the waves travel around the cavity perimeter, the transmission distance becomes longer than in intact wood, resulting in a relatively lower measured velocity (Du et al. 2018; Pahnabi et al. 2024). During this detour, the elastic waves travel at various angles relative to the fiber direction. If the transmission velocity at different angles of fiber direction is known, the wave propagation path can be predicted.

Hankinson's formula (Eq. 1) provides a mathematical relationship to predict compressive strength when a load is applied at an angle between the parallel direction and the perpendicular-to-the-fiber direction in wood. The formula can predict both the strength and the elastic wave velocity according to the fiber orientation angle (Afoutou et al. 2024; Kabir 2001). In this equation, the coefficient *n* represents the degree of anisotropy. For isotropic materials, *n* equals 1, and it increases as anisotropy increases. For wood, *n* must be determined experimentally and typically ranges between 1.5 and 2.5, depending on the tree species (Bachtiar et al. 2017; Mascia et al. 2011; Senalik and Farber 2021).

$$N = \frac{P \times Q}{P \times \sin^n(\theta) + Q \times \cos^n(\theta)} \quad [1]$$

where, N is the predicted elastic wave propagation velocity, P is the wave velocity along the fiber direction (0°), Q is the wave velocity perpendicular to the fiber direction (90°), and θ is the angle of fiber direction.

Red pine (*Pinus densiflora*) has traditionally been used as beams and roof structures in Korean cultural heritage buildings, highlighting its historical and structural relevance. There is currently no established Hankinson's formula coefficient for red pine. To enhance measurement accuracy under varying field moisture conditions, coefficients were determined for moisture levels of 12%, 15%, and 18%.

## Materials and methods

### Materials

#### *Specimen preparation*

Test specimens were prepared by selecting defect-free sections from 81- to 90-year-old pine boards grown in Bonghwa, Gyeongbuk. A total of 15 specimens of 400 × 50 × 400 mm (longitudinal × radial × tangential) were produced. The specific gravity of the specimens was 0.50 ± 0.01.

#### *Moisture content control*

A thermo-hygrostat (Daihan Labtech, LTH-2250C, Namyangju-si, Korea) was used to control the moisture content of the test specimens. To achieve the target moisture contents of 12%,

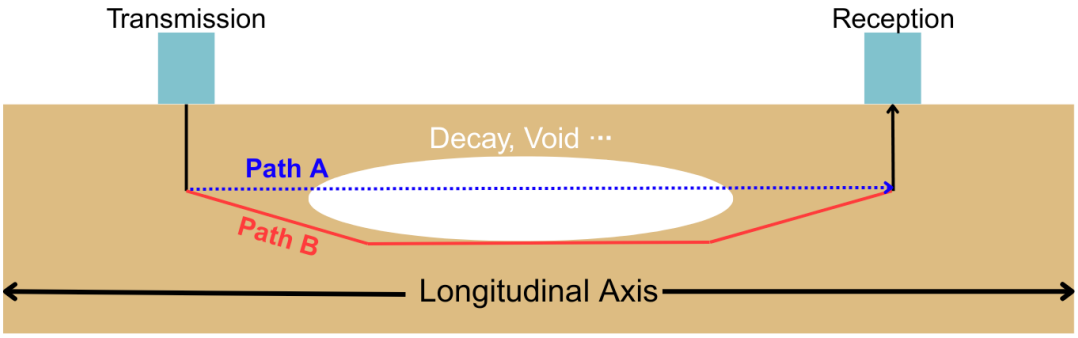


Figure 1. Changes in the path of acoustic wave transmission due to defects.

15%, and 18%, the temperature and relative humidity were set according to the values shown in Table 1 (Kang et al. 2008). The same 15 specimens were used to measure response at each moisture content. The specimens were stored under these controlled conditions until their masses stabilized.

## Methods

### *Measurement angles of fiber direction*

To determine the coefficient for Hankinson's formula, measurements were taken on the wide face at seven angles spaced at 15° intervals from 0° to 90°. The measurement paths, each 300 mm in length, were marked as shown in Figure 2. Here, the fiber direction was defined as 0°, and the direction perpendicular to the fibers was defined as 90°. Prior to testing, all specimens were visually inspected to ensure that the 0° direction was fully aligned with the fiber direction.

### *Indirect elastic wave measurement method*

Elastic wave transmission velocity is calculated by dividing the distance by the time of flight between the transmitter and receiver (Huan et al. 2018; Liang et al. 2010; Wang et al. 2001). Ultrasonic and stress wave measurements were conducted by the indirect method, in which the transmitter and receiver were placed side by side on the surface, as shown in Figure 2 (Nowak et al. 2019). Transmission velocity was measured 30 times for each angle, yielding a total of 210 data sets per specimen. The origin was set at the point where all the angles converge, with the transmitter fixed at this origin and the receiver positioned at the endpoint corresponding to each angle. The transmitter remained stationary when changing angles, and only the receiver was moved.

### *Ultrasonic measurement method.*

The ultrasonic transmission speed was measured using Pundit Lab equipment (Proceq, Pundit Lab, Switzerland) (Figure 3). The frequency of the ultrasonic transmission speed measurement was fixed at 54 kHz (Bucur and Feeney 1992; Espinosa et al. 2019; Tanasoiu et al. 2002).

Table 1. Temperature and relative humidity conditions used to achieve target moisture contents.

| | | Temperature | Relative Humidity |
|---|---|---|---|
| Target Moisture Content | 12% | 20°C | 65% |
| | 15% | 20°C | 77% |
| | 18% | 20°C | 85% |

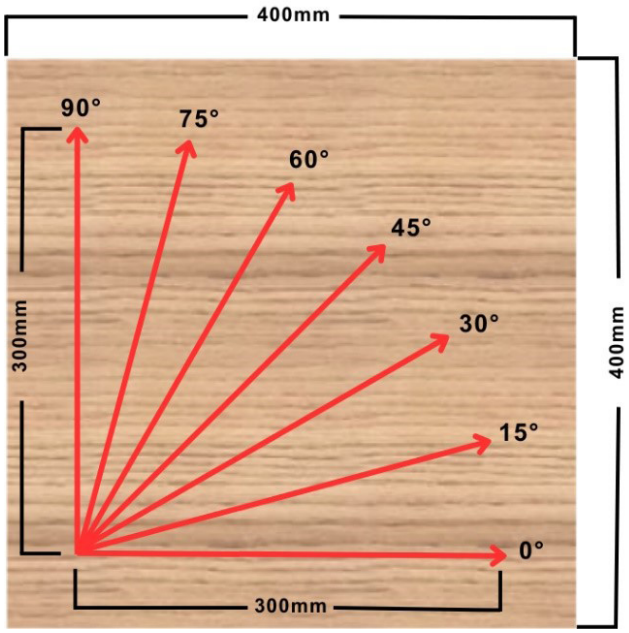


Figure 2. A schematic diagram of a specimen.

The contact surfaces of the measuring terminals were circular with a diameter of 50 mm, and the measurement distance was taken between the centers of the transmitter and receiver. To ensure accurate measurements, ultrasonic couplant (SLTECH, ULTRASONIC COUPLANT, Korea) was applied to the terminals before testing (Fang et al. 2017).

### *Stress wave measurement method*

The stress wave transmission speed was measured using a Micro Hammer device (iML, Micro Hammer, Germany)

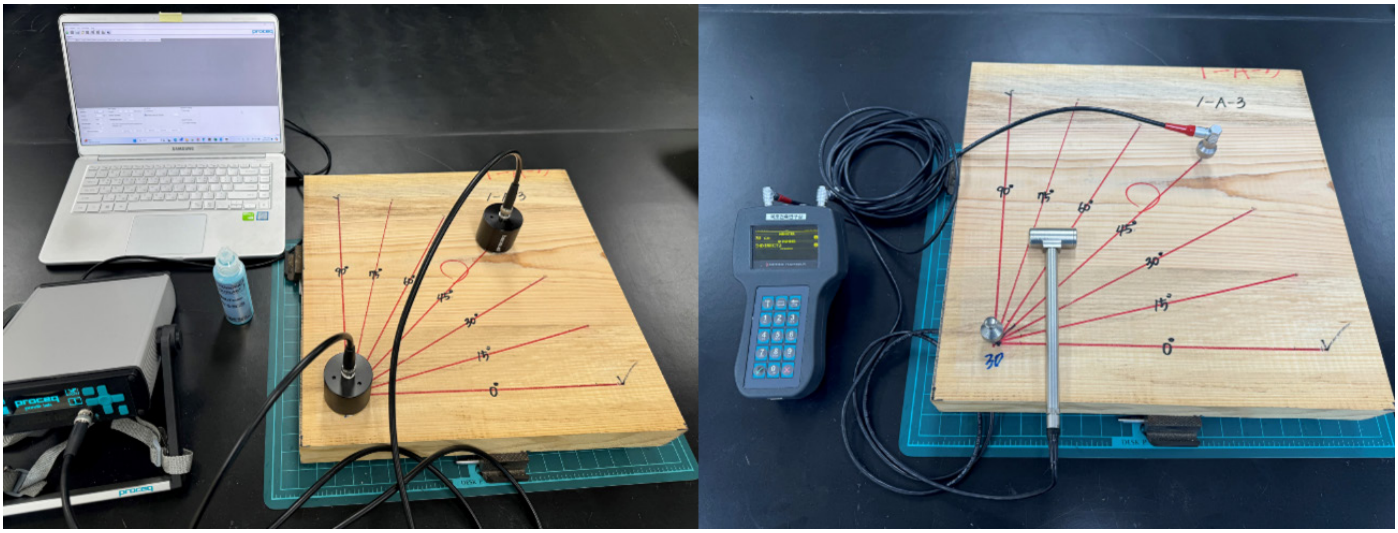

Figure 3. Examples of the ultrasonic wave (left) and stress wave (right) measuring devices on a test sample.

(Figure 3). The measurement involves striking the transmitter with a hammer connected to the device, generating a stress wave that is detected by the receiver. To account for variations in force and angle of striking, three measurements are taken and averaged.

Stress wave transmission velocity was measured by inserting the transmitter and receiver screws into the specimen. The insertion depth was set to 40 mm to ensure the screws were securely fixed and stable during the impact (Wang 1999).

### *Data processing*

A total of 450 data sets per angle were collected from 15 red pine specimens with 30 repetitions each. Since the calculation of coefficient $n$ using the Root Mean Square Error (RMSE) method is highly sensitive to outliers, the data were statistically analyzed to identify and remove outliers, as illustrated in Figure 4 (Shcherbakov et al. 2013).

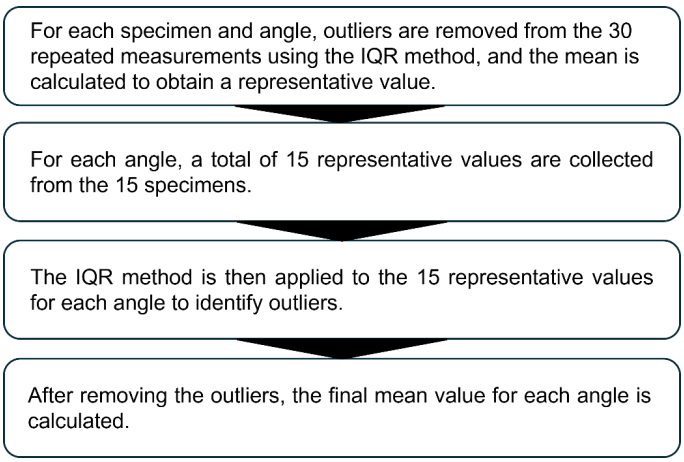


Figure 4. Data handling steps.

### *Outlier removal using IQR method*

The interquartile range (IQR) method identifies outliers based on the central 50% range of the data. The IQR is calculated by subtracting the lower 25th percentile (first quartile, Q1) from the upper 75th percentile (third quartile, Q3), representing the range of the middle 50% of the data. Values lying beyond 1.5 times the IQR below Q1 or above Q3 are considered outliers, and in this study, it was chosen to remove them for increased reliability of the statistical analysis (Danasingh and Leavline 2016). This outlier removal was applied to each set of 30 repetitions, after which the average was calculated. In the case of ultrasonic wave measurements, 0 to 6 outliers were removed per set, whereas for stress wave measurements, 0 to 14 outliers were removed. These 15 mean values, each representing one specimen at a given angle, were then collectively subjected to a second round of IQR-based outlier detection. After removing outliers from this group, the final representative mean for each angle was calculated.

### *Calculating coefficient n using RMSE*

The predicted values were calculated by substituting the actual measured transmission velocities at 0° and 90°, with outliers removed, into Hankinson's formula, where variables $P$ and $Q$ represent the velocities at 0° and 90°, respectively. The angle $\theta$ was set at 15° intervals and converted to radians based on the fiber orientation. The coefficient $n$ was varied from 1.5 to 2.5 in increments of 0.1, and the predicted transmission velocities for ultrasonic and stress waves were calculated accordingly.

To select the most appropriate coefficient $n$, the accuracy of each prediction model was evaluated against the actual measurements using the RMSE. RMSE is a useful statistical measure for assessing the precision of prediction models. The

RMSE formula is provided in Equation 2. The $n$ value with the smallest RMSE was selected as the optimal coefficient.

$$RMSE = \sqrt{\frac{1}{n}\sum_{i=1}^{n}(y_i - \hat{y}_i)^2} \quad [2]$$

where, $n$ is the number of data points, $y_i$ is the measured value, and $\hat{y}_i$ is the predicted value.

### *Evaluating prediction model accuracy using $R^2$ and NRMSE*

The coefficient of determination ($R^2$, Eq 3) measures how well a prediction model explains the actual observed data by comparing the residual sum of squares (SSE) to the total sum of squares (SST). Values closer to 1 indicate a higher explanatory power of the model, while values closer to 0 indicate lower explanatory power.

$$R^2 = 1 - \frac{\sum_{I=1}^{n}(y_i - \hat{y}_i)^2}{\sum_{I=1}^{n}(y_i - \bar{y}_i)^2} \quad [3]$$

where, $y_i$ is the measured value, $\hat{y}_i$ is the predicted value, and $\bar{y}_i$ is the average of the measured values.

Normalized RMSE (NRMSE; Eq 4) is a metric that evaluates the relative accuracy of a model's predictions by normalizing the RMSE value (Shcherbakov et al. 2013). The closer the NRMSE value is to 0, the more closely the predicted values match the actual values, indicating higher prediction accuracy.

$$NRMSE = \frac{RMSE}{X_{max} - X_{min}} \quad [4]$$

where, $X_{max}$ is the maximum value of the data, $X_{min}$ is the minimum value of the data.

## Results and discussion

### *Average velocity of elastic waves under the moisture content variations*

Both ultrasonic and stress wave tests exhibited a consistent trend of decreasing average transmission velocity as the angle increased from 0° to 90° (Figures 5–7). The repeated observation of similar trends under various specimens and moisture conditions provides important evidence supporting the applicability of the indirect measurement method for elastic wave nondestructive testing.

### *Calculating representative values by grain angle*

Table 2 presents the averages and standard deviations of the 15 specimens for each angle after outlier removal, under moisture contents of 12%, 15%, and 18%.

Table 3 shows the elastic wave transmission velocities of ultrasonic and stress waves according to changes in moisture

Table 2. Effect of grain angle on ultrasonic wave and stress wave velocity of red pine at 12% to 18% moisture content.

| | | Velocity(m/s) | | | | | | |
|---|---|---|---|---|---|---|---|---|
| MC | Wave Type | 0° | 15° | 30° | 45° | 60° | 75° | 90° |
| 12% | UW | 5293 | 4530 | 2898 | 1947 | 1579 | 1331 | 1258 |
| | | [194] | [374] | [427] | [454] | [316] | [309] | [273] |
| | SW | 2477 | 2072 | 1564 | 1249 | 1110 | 1018 | 993 |
| | | [135] | [183] | [164] | [145] | [159] | [115] | [69] |
| 15% | UW | 5123 | 4229 | 2597 | 1845 | 1544 | 1289 | 1233 |
| | | [191] | [400] | [468] | [457] | [289] | [309] | [238] |
| | SW | 2414 | 2037 | 1489 | 1201 | 1071 | 976 | 960 |
| | | [135] | [165] | [146] | [147] | [138] | [105] | [64] |
| 18% | UW | 5070 | 4183 | 2761 | 1784 | 1443 | 1228 | 1222 |
| | | [272] | [388] | [255] | [411] | [307] | [273] | [223] |
| | SW | 2374 | 1935 | 1435 | 1158 | 1023 | 941 | 933 |
| | | [76] | [191] | [150] | [142] | [147] | [97] | [79] |

Values represent the mean of samples, while tables in brackets represent the standard deviation.

Table 3. Average change in acoustic wave transfer velocity after outlier removal due to change in moisture content.

| Average | MC | 0° | 15° | 30° | 45° | 60° | 75° | 90° |
|---|---|---|---|---|---|---|---|---|
| UW | 12% | 5293 | 4530 | 2898 | 1947 | 1579 | 1331 | 1258 |
| | 15% | 5123 | 4229 | 2597 | 1845 | 1544 | 1289 | 1233 |
| | 18% | 5070 | 4183 | 2761 | 1784 | 1443 | 1228 | 1222 |
| SW | 12% | 2477 | 2072 | 1564 | 1249 | 1110 | 1018 | 993 |
| | 15% | 2414 | 2037 | 1489 | 1201 | 1071 | 976 | 960 |
| | 18% | 2374 | 1935 | 1435 | 1158 | 1023 | 941 | 933 |

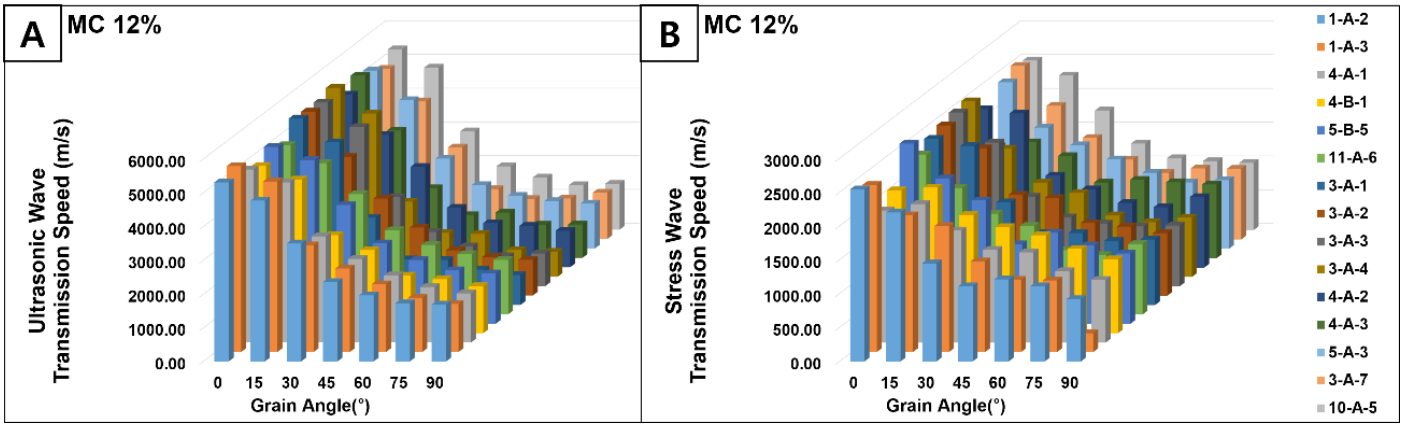


Figure 5. Effect of grain angle on transmission speed of ultrasonic waves (A) and stress waves (B) at 12% moisture content.

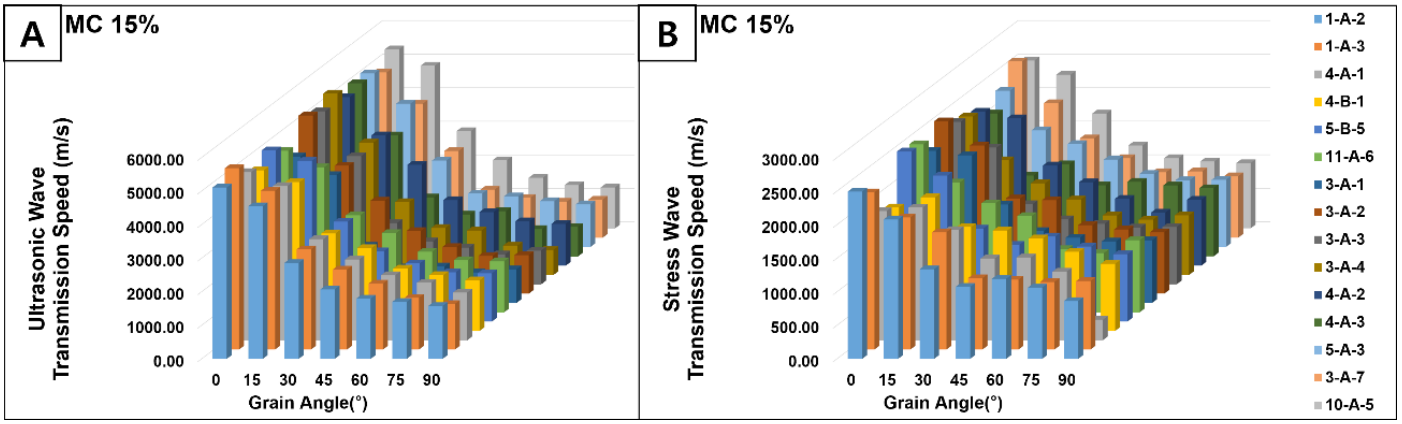


Figure 6. Effect of grain angle on transmission speed of ultrasonic waves (A) and stress waves (B) at 15% moisture content.

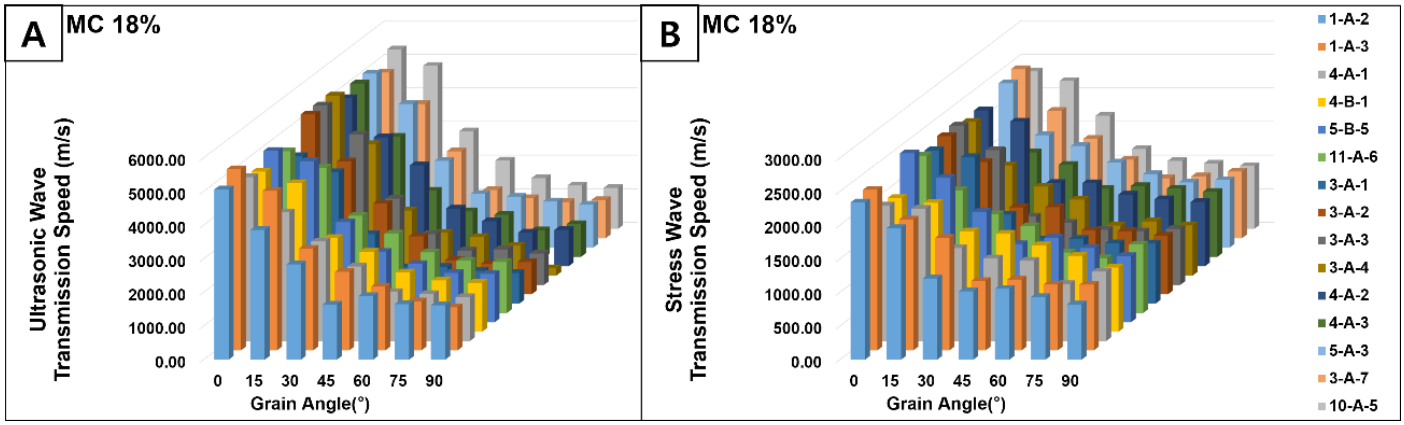


Figure 7. Effect of grain angle on transmission speed of ultrasonic waves (A) and stress waves (B) at 18% moisture content.

content and fiber orientation angle. Average transmission speed decreased as the angle increased from 0° to 90°. This behavior is attributed to the anisotropic nature of wood, where elastic waves propagate through cell walls. At 0°, fibers are long and most aligned, resulting in a relatively shorter transmission path. At 90°, the cell walls are densely arranged nearly perpendicular to the wave path, creating a longer transmission path, increased transmission time, and thus lower speed (Espinosa et al. 2019; Li et al. 2021).

### *Comparison of predicted and measured values according to changes in coefficients of Hankinson's formula*

The results comparing the predicted and measured values for different values of n are presented in Figures 8 to 10.

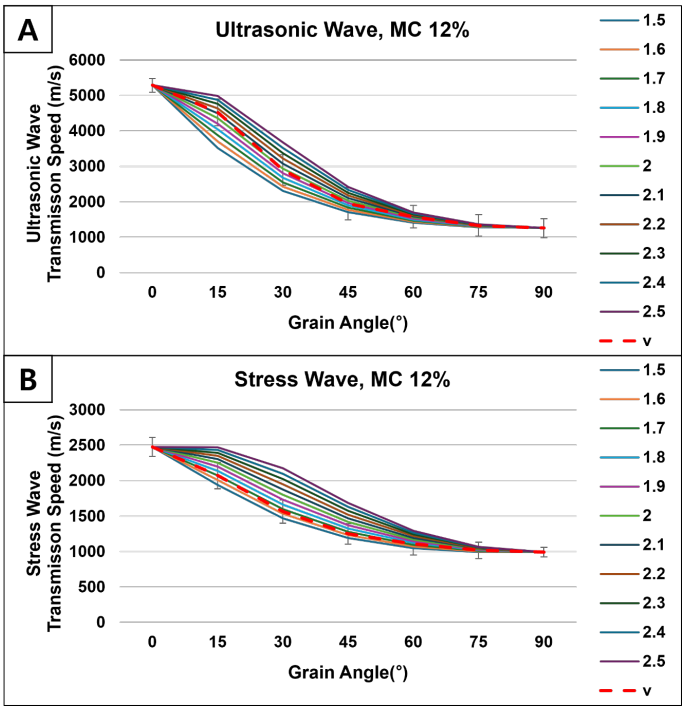


Figure 8. Effect of coefficient *n* on transmission speed of ultrasonic waves (A) and stress waves (B) in wood at 12% moisture content.

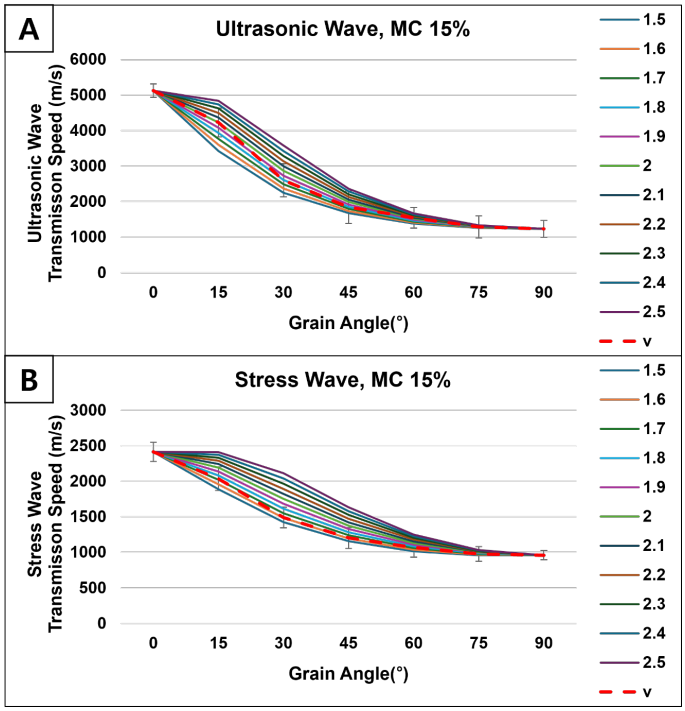


Figure 9. Effect of coefficient *n* on transmission speed of ultrasonic waves (A) and stress waves (B) in wood at 15% moisture content.

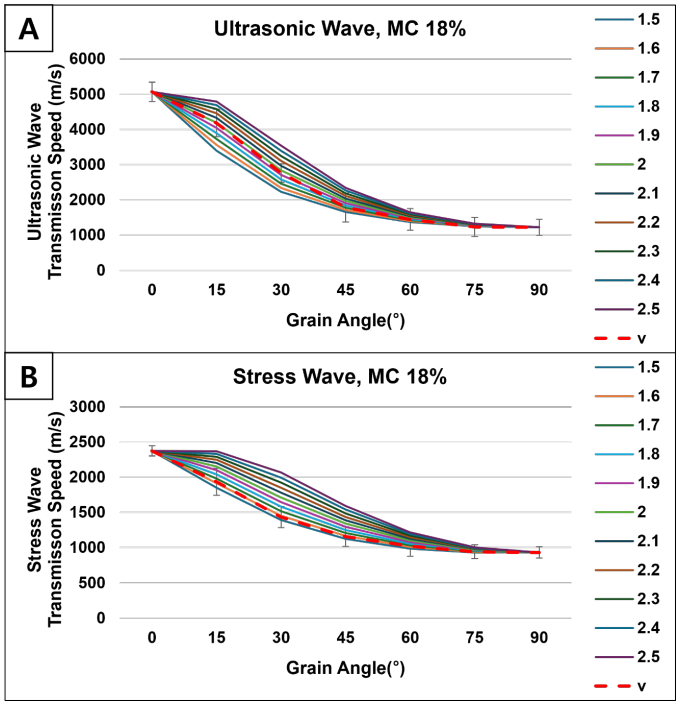


Figure 10. Effect of coefficient *n* on transmission speed of ultrasonic waves (A) and stress waves (B) in wood at 18% moisture content.

The measured ultrasonic and stress wave transmission velocities at moisture contents of 12%, 15%, and 18% are represented by v, while the predicted values corresponding to coefficient *n* varying from 1.5 to 2.5 are shown as thin solid lines.

### *Results of adopting coefficient n using RMSE*

Based on the predicted and measured values shown in Figures 8 to 10, the RMSE was calculated to compare the errors of each prediction model as the coefficient *n* varied. The results are summarized in Table 4, and the coefficient *n* with the lowest RMSE was selected as the optimal value for each moisture content, ultrasonic wave, and stress wave.

Table 4. Effect of varying the coefficient n on RMSE in ultrasonic and stress wave analysis of red pine under different moisture content conditions.

| | MC 12% | | MC 15% | | MC 18% | |
|---|---|---|---|---|---|---|
| *n* | UW | SW | UW | SW | UW | SW |
| 1.5 | 455.60 | 70.60 | 343.44 | 68.39 | 364.81 | 40.84 |
| 1.6 | 370.72 | 31.55 | 262.91 | 33.93 | 284.51 | *11.39 |
| 1.7 | 287.10 | *17.65 | 185.75 | *28.29 | 206.22 | 40.06 |
| 1.8 | 205.81 | 53.41 | 117.76 | 59.56 | 132.71 | 77.57 |
| 1.9 | 129.99 | 92.48 | *82.91 | 96.60 | *76.56 | 115.34 |
| 2.0 | *75.12 | 131.79 | 114.54 | 134.56 | 82.98 | 153.04 |
| 2.1 | 90.43 | 171.13 | 179.45 | 172.79 | 142.44 | 190.66 |
| 2.2 | 155.27 | 210.49 | 252.49 | 211.15 | 213.82 | 228.25 |
| 2.3 | 230.48 | 249.94 | 327.83 | 249.64 | 287.92 | 265.89 |
| 2.4 | 308.20 | 289.55 | 403.95 | 288.32 | 362.81 | 303.65 |
| 2.5 | 386.78 | 329.40 | 480.40 | 327.23 | 438.01 | 341.61 |

* The smallest value as a result of RMSE calculation. Adopt the corresponding coefficient *n*.

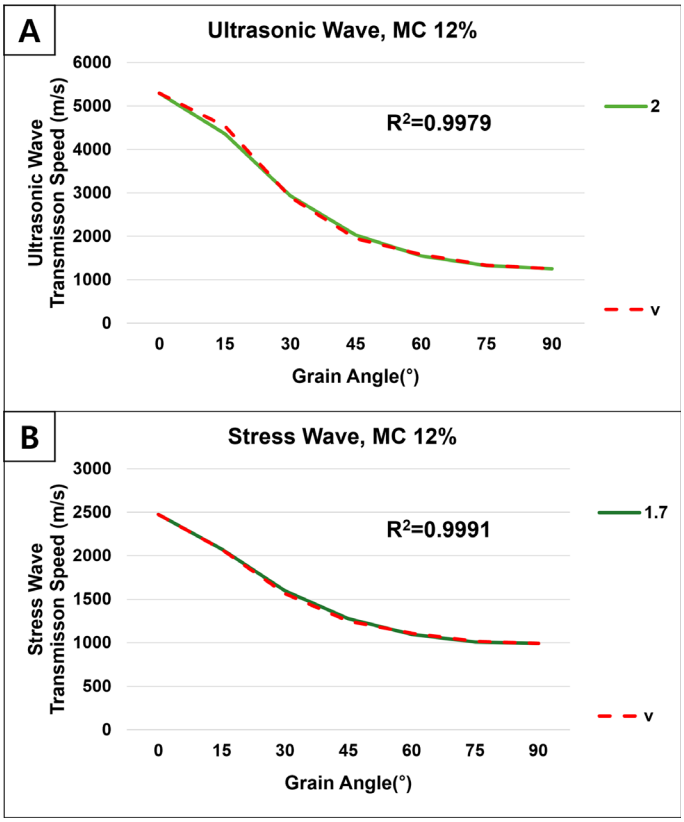


Figure 11. Effect of grain angle on stress wave and ultrasonic wave transmission speed when the coefficient calculation uses RMSE for wood at 12% moisture content.

The values marked with * in Table 4 indicate the cases where the RMSE between the predicted and measured values was the smallest. The corresponding coefficient *n* was adopted as the optimal value for each condition. For moisture contents of 12%, 15%, and 18%, the optimal *n* values were 2.0, 1.9, and 1.9 for ultrasonic waves, and 1.7, 1.7, and 1.6 for stress waves, respectively.

### *Results of evaluating the accuracy of the prediction model using $R^2$ and NRMSE*

As moisture content increased, both wave types showed decreasing transmission velocities and lower *n* values, indicating a reduction in anisotropy within the wood.

By substituting the optimal coefficient *n*, Hankinson's formula for red pine was established for each moisture content condition (12%, 15%, and 18%). The predicted and measured values for each angle based on this formula are presented in Figures 11 to 13.

The coefficients of determination ($R^2$) were all very close to 1, indicating that the prediction model based on the adopted coefficient *n* explains the actual values very well. Additionally, the NRMSE results for ultrasonic and stress waves under the same conditions are presented in Table 5. In all cases, the

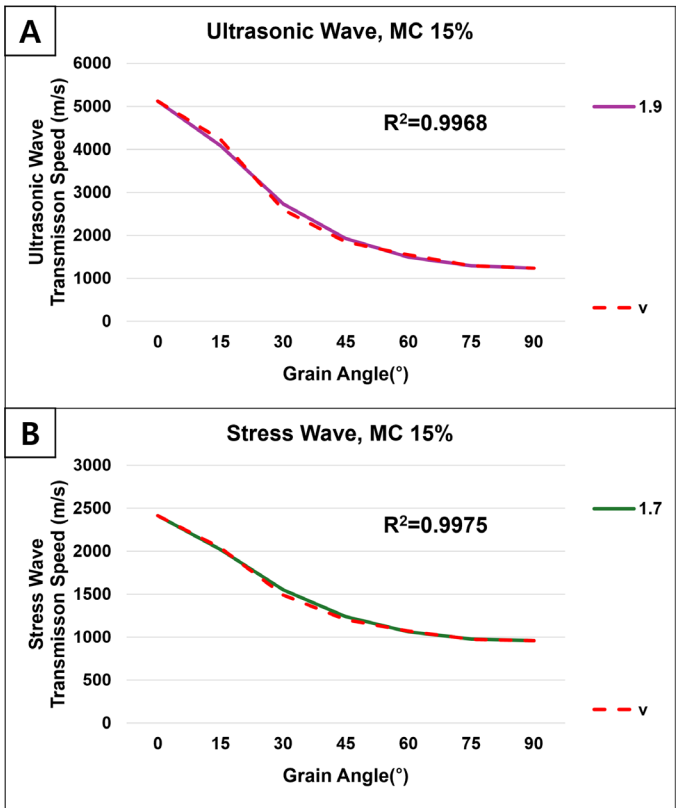


Figure 12. Effect of grain angle on stress wave and ultrasonic wave transmission speed when the coefficient calculation uses RMSE for wood at 15% moisture content.

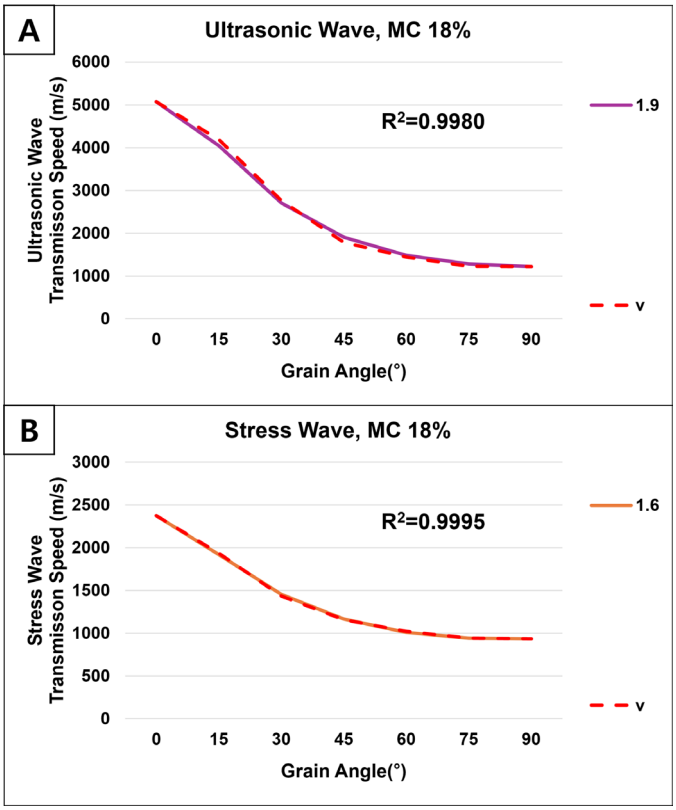


Figure 13. Effect of grain angle on stress wave and ultrasonic wave transmission speed when the coefficient calculation uses RMSE for wood at 18% moisture content.

Table 5. Predictive model accuracy evaluation results using NRMSE.

| MC | | *n* | NRMSE |
|---|---|---|---|
| 12% | UW | 2.0 | 0.0186 |
| | SW | 1.7 | 0.0120 |
| 15% | UW | 1.9 | 0.0213 |
| | SW | 1.7 | 0.0199 |
| 18% | UW | 1.9 | 0.0199 |
| | SW | 1.6 | 0.0081 |

NRMSE values ranged between 0 and 0.1, confirming that the completed Hankinson's formula had high prediction accuracy.

As shown in Table 5, the coefficient *n* gradually decreases with increasing moisture content. This occurs because higher moisture content enhances the viscoelastic effects within the wood, leading to a more uniform mechanical stiffness as moisture penetrates the cell structure (Eitelberger et al. 2012).

These changes reduce the anisotropy of the wood, which consequently lessens the variation in elastic wave propagation velocity with angle. This effect is reflected as a flatter slope in the angle-velocity graphs shown in Figures 14 and 15. Therefore, this reduction in anisotropy caused the coefficient *n* in Hankinson's formula to decrease.

### *Determining the effect of function ratio on elastic wave propagation speed*

Ultrasonic waves consistently exhibited higher transmission velocities than stress waves, which is consistent with the findings of Chuang and Wang (2001). This trend was observed across most moisture content conditions and specimens, providing experimental support for the applicability of Hankinson's formula.

Figure 14 shows the change in transmission speed according to varying moisture content for ultrasonic waves, while Figure 15 illustrates the change in transmission speed for stress waves under different moisture content levels.

As the moisture content of the specimen increased from 12% to 18%, the elastic wave propagation velocity showed an overall decreasing trend, with a reduction of approximately 3% to 10% at each angle, as shown in Figure 16.

Generally, the propagation velocity of elastic waves increases when the increase in elastic modulus outweighs the increase in density. However, below the fiber saturation point, as the moisture content increases, density increases while the elastic modulus decreases, resulting in a decrease in elastic wave velocity (Liu et al. 2014; Montero et al. 2015).

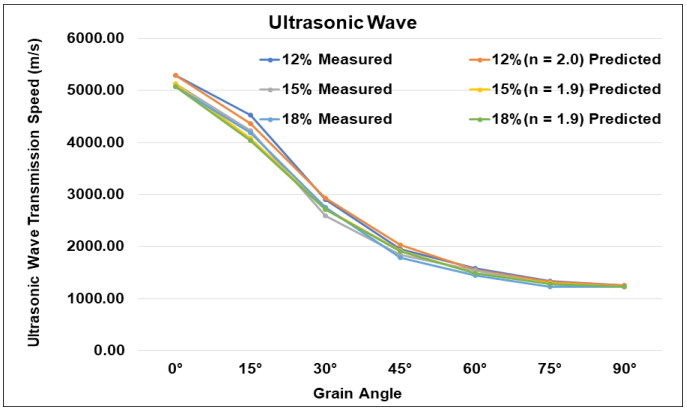


Figure 14. Effect of wood moisture content on ultrasonic wave transmission speed measured at different grain angles, including comparison between measured and predicted values.

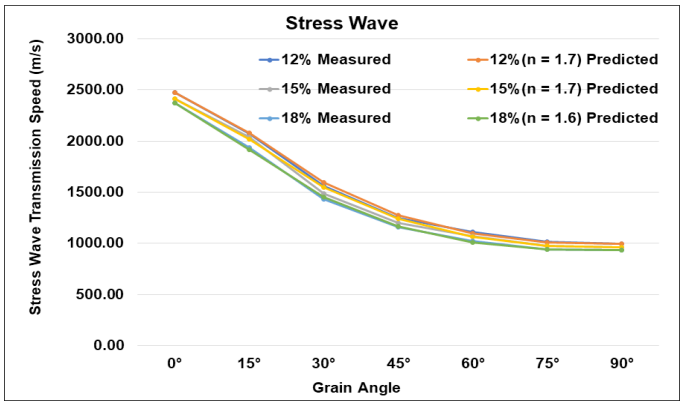


Figure 15. Effect of wood moisture content on stress wave transmission speed measured at different grain angles, including comparison between measured and predicted values.

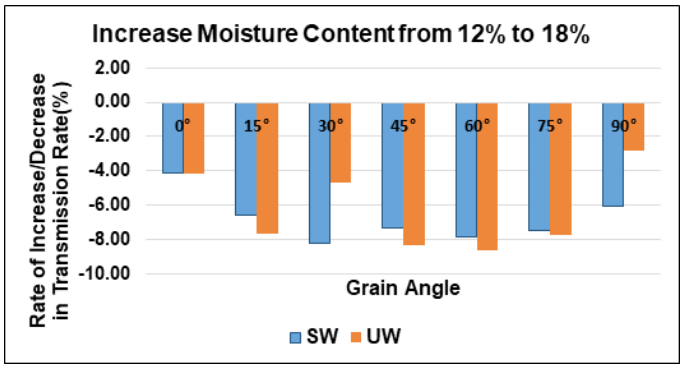


Figure 16. Effect of grain angle and wood moisture content on the velocities of ultrasonic and stress waves in red pine.

## Conclusions

As moisture content increased, elastic wave velocity decreased, with ultrasonic waves consistently exhibiting higher velocities than stress waves. The optimal coefficient *n* in Hankinson's formula was identified for each moisture level, allowing for the development of a predictive model specific to red pine.

While stress wave velocities were much lower than ultrasonic wave velocities, Hankinson's formula effectively predicted both types of velocities across a range of grain angles and varying moisture conditions. These findings support the applicability of the formula in nondestructive testing (NDT) for evaluating wave propagation in moisture-affected wood. The methodology presented in this study may be repeatable with other wood species, suggesting broader applicability of Hankinson's formula in the field of NDT.

## Acknowledgments

This research was supported by the Korea Heritage Service through the R&D project, "Development and verification of technology for aged wood recovery from architectural cultural heritage in response to climate damage" (Project No. RS-2024-000403459).

## References

Afoutou JS, Zhang X, Dubois F (2024) Full elastic properties characterization of wood by ultrasound using a single sample. Wood Sci Technol 58:403–422. https://doi.org/10.1007/s00226-023-01525-y

Azzi Z, Al Sayegh H, Metwally O, Eissa M (2025) Review of nondestructive testing (NDT) techniques for timber structures. Infrastructures 10(2):28. https://doi.org/10.3390/infrastructures10020028

Bachtiar EV, Rüggeberg M, Hering S, Kaliske M, Niemz P (2017) Estimating shear properties of walnut wood: A combined experimental and theoretical approach. Mater Struct 50:248. https://doi.org/10.1617/s11527-017-1119-2

Bucur V, Feeney FE (1992) Attenuation of ultrasound in solid wood. Ultrasonics 30:76–81. https://api.semanticscholar.org/CorpusID:122875380

Buczkowski G, Bertelsmeier C (2017) Invasive termites in a changing climate: A global perspective. Ecol Evol 7:974–985. https://doi.org/10.1002/ece3.2674

Chuang ST, Wang SY (2001) Evaluation of standing tree quality of Japanese cedar grown with different spacing using stress-wave and ultrasonic-wave methods. J Wood Sci 47:245–253. https://doi.org/10.1007/BF00766709

Churkina G, Organschi A, Reyer CPO, Ruff A, Vinke K, Liu Z, Reck BK, Graedel TE, Schellnhuber HJ (2020) Buildings as a global carbon sink. Nat Sustain 3(4):269–276. https://doi.org/10.1038/s41893-019-0462-4

Danasingh AA, Leavline JE (2016) Model-based outlier detection system with statistical preprocessing. J Mod Appl Stat Methods 15(1):789–801. https://doi.org/10.22237/jmasm/1462077480

Du X, Li J, Feng H, Chen S (2018) Image reconstruction of internal defects in wood based on segmented propagation rays of stress waves. Appl Sci 8(10):1778. https://doi.org/10.3390/app8101778

Eitelberger J, Bader T, De BorstK, Jäger A (2012) Multiscale prediction of viscoelastic properties of softwood under constant climatic conditions. Comput Mater Sci 55:303–312. https://doi.org/10.1016/j.commatsci.2011.11.033

Espinosa L, Prieto F, Brancheriau L, Lasaygues P (2019) Effect of wood anisotropy in ultrasonic wave propagation: A ray-tracing approach. Ultrasonics 91:242–251. https://doi.org/10.1016/j.ultras.2018.07.015

Fang Y, Lin L, Feng H, Emms GW, Lu Z (2017) Review of the use of air-coupled ultrasonic technologies for nondestructive testing of wood and wood products. Comput Electron Agric 137:79–87. https://doi.org/10.1016/j.compag.2017.03.015

Ghaly A, Edwards S (2011) Termite damage to buildings: Nature of attacks and preventive construction methods. Am J Eng Appl Sci 4(2):187–200. https://doi.org/10.3844/ajeassp.2011.187.200

Huan Z, Jiao Z, Li G, Wu X (2018) Velocity error correction based tomographic imaging for stress wave nondestructive evaluation of wood. BioResources 13(2):2530–2545. https://doi.org/10.15376/biores.13.2.2530-2545

Kabir MF (2001) Prediction of ultrasonic properties from grain angle. J Inst Wood Sci 15(5):235–246.

Kang C, Kim N, Kim B, Kim Y, Byun H, So W, Yeo H, Oh S, Lee W, Lee H (2008) Introduction to Wood Physics and Mechanics. Hyangmunsa, Seoul. 338 p.

Kim GC, Bae MS, Lee JJ (2003) Difference of deterioration according to exposed condition of column in wooden traditional building. J Korean Wood Sci Technol 31(2):58–68.

Kretschmann DE (2010) Mechanical properties of wood. Chapter 5 in Wood handbook: Wood as an engineering material, Centennial ed., General Technical Report FPL-GTR-190. USDA Forest Service Forest Prod Lab, Madison, WI. https://www.fpl.fs.usda.gov/documnts/fplgtr/fplgtr190/chapter_05.pdf

Lee S-B, Tong RL, Kim S-H, Im I-G, Su N-Y (2021). Potential pest status of the Formosan subterranean termite, *Coptotermes formosanus* Shiraki (Blattodea: Isoptera: Rhinotermitidae), in response to climate change in the Korean Peninsula. Fla Entomol 103(4):431–437. https://doi.org/10.1653/024.103.00403

Li M, Wang M, Ding R, Deng T, Fang S, Lai F, Luoi R (2021) Study of acoustic emission propagation characteristics and energy attenuation of surface transverse wave and internal longitudinal wave of wood. Wood Sci Technol 55(6):1619–1637. https://doi.org/10.1007/s00226-021-01329-y

Liang S, Fu F, Lin L, Hu N (2010) Various factors and propagation trends of stress waves in cross sections of Euphrates poplar. For Prod J 60(5):440–446. https://meridian.allenpress.com/fpj/article-pdf/60/5/440/1698790/0015-7473-60_5_440.pdf

Liu H, Gao J, Chen Y, Liu Y (2014) Effects of moisture content and fiber proportion on stress wave velocity in Cathay poplar (*Populus cathayana*) wood. BioResources 9(2):2214–2226. https://bioresources.cnr.ncsu.edu/resources/effects-of-moisture-content-and-fiber-proportion-on-stress-wave-velocity-in-cathay-poplar-populus-cathayana-wood/

Mascia N, Nicolas EA, Todeschini R (2011) Comparison between Tsai-Wu failure criterion and Hankinson's formula for tension in wood. Wood Res 56(4):499-510.

Montero MJ, de La Mata J, Esteban M, Hermoso E (2015) Influence of moisture content on the wave velocity to estimate mechanical properties of large cross-section Scots pine. Maderas. Ciencia y tecnología 17(2):407–420. https://www.scielo.cl/scielo.php?pid=S0718-221X2015005000038&script=sci_arttext&tlng=en

Niederleithinger E, Vössing KJ (2018) Nondestructive assessment and imaging methods for internal inspection of timber: A review. Holzforschung 72(6):467–476. https://doi.org/10.1515/hf-2017-0122

Nowak T, Karolak A, Sobótka M, Wyjadłowski M (2019) Assessment of the condition of wharf timber sheet wall material by means of selected non-destructive methods. Materials 12(9):1532. https://doi.org/10.3390/ma12091532

Ondrejka V, Gergeľ T, Bucha T, Pástor M (2020) Innovative methods of non-destructive evaluation of log quality. Cent Eur For J 66, 1–11. https://doi.org/10.2478/forj-2020-0021

Pahnabi N, Schumacher T, Sinha A (2024) Imaging of structural timber based on in situ radar and ultrasonic wave measurements: A review of the state-of-the-art. Sensors 24(9):2901. https://doi.org/10.3390/s24092901

Riggio M, Anthony RW, Augelli F, Kasal B, Lechner T, Muller W, Tannert T (2014) In situ assessment of structural timber using non-destructive techniques. Mater Struct 47:749–766. https://doi.org/10.1617/s11527-013-0093-6

Senalik CA, Farber B (2021). Mechanical properties of wood. Chapter 5 in Wood handbook: Wood as an engineering material, General Technical

Report FPL-GTR-282. USDA Forest Service Forest Prod Lab, Madison, WI, 46 p. https://research.fs.usda.gov/treesearch/62244

Shabani A, Kioumarsi M, Plevris V, Stamatopoulos H (2020) Structural vulnerability assessment of heritage timber buildings: A methodological proposal. Forests 11(8):881. https://doi.org/10.3390/f11080881

Shcherbakov M, Brebels A, Shcherbakova NL, Tyukov A, Janovsky TA, Kamaev VA (2013) A survey of forecast error measures. World Appl Sci J 24(24):171–176. https://www.researchgate.net/publication/281718517_A_survey_of_forecast_error_measures

Starzyk A, Rybak-Niedziółka K, Nowysz A, Marchwiński J, Kozarzewska A, Koszewska J, Piętocha A, Vietrova P, Łacek P, Donderewicz M, Langie K, Walasek K, Zawada K, Voronkova I, Francke B, Podlasek A (2024) New zero-carbon wooden building concepts: A review of selected criteria. Energies 17(17):4502. https://doi.org/10.3390/en17174502

Tanasoiu V, Miclea C, Tanasoiu C (2002) Nondestructive testing techniques and piezoelectric ultrasonics transducers for wood and built-in wooden structures. JOAM 4(4):949–957.

Verbist M, Nunes L, Jones D, Branco JM (2019) Service life design of timber structures, in Long-term Performance and Durability of Masonry Structures: Degradation Mechanisms, Health Monitoring and Service Life Design, ed B Ghiassi, P B Lourenço. Woodhead Publishing, Duxford, UK, pp. 311–336. https://www.sciencedirect.com/science/article/pii/B978008102110100011X

Wang JY, Stirling R, Morris P, Taylor A, Lloyd J, Kirker G, Lebow S, Mankowski M, Barnes HM, Morrell JJ (2018) Durability of mass timber structures: A review of the biological risks. Wood Fiber Sci 50:110–127. https://doi.org/10.22382/wfs-2018-045

Wang X, Ross RJ, McClellan M, Barbour RJ, Erickson JR, Forsman JW, McGinnis GD (2001) Nondestructive evaluation of standing trees with a stress wave method. Wood Fiber Sci 33(4):522–533. http://wfs.swst.org/index.php/wfs/article/view/1014

Wang X (1999) Stress wave-based nondestructive evaluation (NDE) methods for wood quality of standing trees. ProQuest Diss Theses. https://search.proquest.com/openview/5c7470d4496f6503c6fd0c44cd8ddbc1/1?pq-origsite=gscholar&cbl=18750&diss=y

Yang H, Yu L, Wang L (2015) Effect of moisture content on the ultrasonic acoustic properties of wood. J For Res 26(3):753–757. https://doi.org/10.1007/s11676-015-0079-z

Zielińska M, Rucka M (2021) Non-destructive testing of wooden elements. IOP Conference Series: Materials Science and Engineering 1203:032058. https://doi.org/10.1088/1757-899X/1203/3/032058